Inorg. Chem. **2002**, *41*, 1862–1869

Self-Assembly of Transition-Metal-Based Macrocycles Linked by Photoisomerizable Ligands: Examples of Photoinduced Conversion of Tetranuclear–Dinuclear Squares

Shih-Sheng Sun, Jason A. Anspach, and Alistair J. Lees*

Department of Chemistry, State University of New York at Binghamton, Binghamton, New York 13902-6016

Received September 25, 2001

A series of hetero- and homometallic square complexes bridged by a photoactive 4,4′-azopyridine (AZP) or 1,2-bis(4-pyridyl)ethylene (BPE) ligand, cyclobis{[*cis*-(dppf)M](μ-L)$_2$(*fac*-Re(CO)$_3$Br)}(OTf)$_4$ (M = Pd, L = *trans*-AZP (**5**); M = Pt, L = *trans*-AZP (**7**); M = Pd, L = *trans*-BPE (**8**); M = Pt, L = *trans*-BPE (**10**)), cyclo{[*cis*-(dppf)M]-(μ-L)$_2$(*fac*-Re(CO)$_3$Br)}(OTf)$_2$ (M = Pd, L = *cis*-AZP (**6**); M = Pd, L = *cis*-BPE (**9**)), [*cis*-(dppf)Pd(μ-*trans*-AZP)]$_4$-(OTf)$_8$ (**11**), and [*cis*-(dppf)Pd(μ-*cis*-AZP)]$_2$(OTf)$_4$ (**12**), where dppf is 1,1′-bis(diphenylphosphino)ferrocene and OTf is trifluoromethanesulfonate anion, were prepared by thermodynamically driven self-assembly processes. The photophysical and photochemical properties of these complexes have been investigated, and all of them show a lack of luminescence in room temperature solution. Upon irradiation at 313 or 366 nm, Pd(II)–Re(I)-containing tetranuclear squares **5**, **8**, and **11** undergo photoisomerization and convert to their corresponding dinuclear complexes **6**, **9**, and **12**, whereas Pt(II)–Re(I)-based squares **7** and **10** show only slow square disassembling processes. The tetranuclear squares can be fully recovered by heating the photoisomerized solution for several hours.

Introduction

Thermodynamically driven self-assembly processes have been recognized as one of the most efficient ways to produce structurally well-defined and complex molecular entities from constituent components in solution.[1] The incorporation of photoactive components into the molecular structure, which allows reversible switching of the output physical properties by an external trigger, such as light or redox potential, has attracted great interest because of their potential applications in the further development of molecular or supramolecular devices.[2]

Azobenzene[3] or stilbene[4] and their derivatives are known to undergo efficient reversible photoisomerization reactions. Typically, the thermodynamically stable *trans* isomer can be switched to the *cis* form by UV-light irradiation, and this can then be converted back to the *trans* form by heating or exposure to visible light. Thus, azobenzene and stilbene moieties have been used to construct many interesting photoresponsive molecular systems.[3,5] Although the isomerization processes of azobenzene and stilbene have been studied for almost four decades, the isomerization properties of transition-metal complexes comprising azo-containing or stilbene-like ligands are much less known.[6,7] Herein, we

* To whom correspondence should be addressed. E-mail: alees@binghamton.edu.

(1) (a) Swiegers, G. F.; Malefetse, T. J. *Chem. Rev.* **2000**, *100*, 3483 and references therein. (b) Leininger, S.; Olenyuk B.; Stang, P. J. *Chem. Rev.* **2000**, *100*, 853 and references therein.
(2) Lehn, J.-M. *Supramolecular Chemistry*; VCH Publishers: New York, 1995.
(3) Balzani V.; Scandola, F. *Supramolecular Photochemistry*; Ellis Horwood Ltd.: Chichester, England, 1991; Chapter 7 and references therein.
(4) Görner, H.; Kuhn, H. J. *Adv. Photochem.* **1995**, *19*, 1 and references therein.
(5) Meier, H. *Angew. Chem., Int. Ed. Engl*. **1992**, *31*, 1399 and references therein.
(6) (a) Sun, S.-S.; Lees, A. J. *J. Am. Chem. Soc*. **2000**, *122*, 8956. (b) Yutaka, T.; Kurihara, M.; Kubo K.; Nishihara, H. *Inorg. Chem*. **2000**, *39*, 3438. (c) Tsuchiya, S. *J. Am. Chem. Soc*. **1999**, *121*, 48. (d) Otsuki, J.; Harada K.; Araki, K. *Chem. Lett*. **1999**, 269. (e) Hayami, S.; Inoue, K.; Osaki S.; Maeda, Y. *Chem. Lett*. **1998**, 987. (f) Yam, V. W.-W.; Lau, V. C.-Y.; Wu, L.-X. *J. Chem. Soc., Dalton Trans.* **1998**, 1461. (g) Kurihara, M.; Matsuda, T.; Hirooka, A.; Yutaka, T.; Nishihara, H. *J. Am. Chem. Soc*. **2000**, *122*, 12373. (h) Wakatsuki, Y.; Yamazaki, H.; Grutsch, P. A.; Santhanam, M.; Kutal, C. *J. Am. Chem. Soc*. **1985**, *107*, 8153. (i) Otsuki, J.; Tsujino, M.; Iizaki, T.; Araki, K.; Seno, M.; Takatera, K.; Watanabe, T. *J. Am. Chem. Soc*. **1997**, *119*, 7895. (j) Yutaka, T.; Mori, I.; Kurihara, M.; Mizutani, J.; Kubo K.; Furusho, S.; Matsumura, K.; Tamai, N.; Nishihara, H. *Inorg. Chem*. **2001**, *40*, 4986. (k) Yam, V. W.-W.; Yang, Y.; Zhang, J.; Chu, B. W.-K.; Zhu, N. *Organometallics* **2001**, *20*, 4911.

10.1021/ic010998e CCC: $22.00
Published on Web 03/07/2002

describe the preparation and photochemistry of a series of self-assembly transition-metal-based macrocyclic compounds bridged by a photoisomerizable 4,4′-azopyridine (AZP) or 1,2-bis(4-pyridyl)ethylene (BPE) ligand. The results show that some of the complexes undergo photoinduced and thermally reversible isomerization, which is directly related to the lability of the metal centers.

Experimental Section

Materials and General Procedures. All reactions and manipulations were carried out under N_2 or Ar with the use of standard inert-atmosphere and Schlenk techniques. Solvents used for synthesis were dried by standard procedures and stored under N_2. Solvents used in photolysis were spectroscopic grade. The compounds [*cis*-M(dppf)$(H_2O)_2$](OTf)$_2$ (M is Pd or Pt, dppf is 1,1′-bis(diphenylphosphino)ferrocene, and OTf is trifluoromethanesulfonate anion),[8] *fac*-BrRe(CO)$_3$(*trans*-AZP)$_2$ (**1**),[6a] *fac*-BrRe(CO)$_3$(*trans*-BPE)$_2$ (**2**),[9] *cis*-AZP,[10] *cis*-BPE,[11] and BrRe(CO)$_3$(THF)$_2$[12] were prepared according to published procedures.

Syntheses. All syntheses and purifications were performed in the dark under red light to avoid undesired isomerization.

***fac*-BrRe(CO)$_3$(*cis*-AZP)$_2$ (3)**. To a 100 mL flask containing 460 mg (2.5 mmol) of *cis*-AZP and 123 mg (0.24 mmol) of *fac*-BrRe(CO)$_3$(THF)$_2$ was added 50 mL of dried THF, and the resulting mixture was stirred at room temperature in the dark under nitrogen for 15 min. The solution volume was reduced to ∼20 mL, and subsequently 100 mL of cold ether was added to precipitate the orange product. The resulting precipitate was collected on a frit, washed with cold ether, and dried in vacuo to afford powdery **3**. Yield: 87%. IR (ν_{CO}, cm^{-1}, CH_2Cl_2): 2028, 1931, 1896. ^{1}H NMR (acetone-d_6): 9.10 (d, 4 H, $^3J_{H-H}$ = 6.8 Hz, H$_\alpha$-PyRe), 8.64 (d, 4 H, $^3J_{H-H}$ = 6.8 Hz, H$_\alpha$-Py), 7.72 (d, 4 H, $^3J_{H-H}$ = 6.8 Hz, H$_\beta$-PyRe), 6.86 (d, 4 H, $^3J_{H-H}$ = 6.9 Hz, H$_\beta$-Py). Anal. Calcd for $C_{23}H_{16}N_8BrO_3Re$: C, 38.45; H, 2.25; N, 15.59. Found: C, 38.01; H, 2.69; N, 15.43.

***fac*-BrRe(CO)$_3$(*cis*-BPE)$_2$ (4)**. To a 100 mL flask containing 455 mg (2.5 mmol) of *cis*-BPE and 123 mg (0.24 mmol) of *fac*-BrRe(CO)$_3$(THF)$_2$ was added 50 mL of dried THF, and the resulting mixture was stirred at room temperature in the dark under nitrogen for 15 min. The solution volume was reduced to ∼20 mL, and subsequently 100 mL of cold ether was added to precipitate the orange product. The resulting precipitate was collected on a frit, washed with cold ether, and dried in vacuo to afford a yellow powder. Yield: 79%. IR (ν_{CO}, cm^{-1}, CH_2Cl_2): 2025, 1925, 1890. ^{1}H NMR (CD_2Cl_2): 8.59 (d, 4 H, $^3J_{H-H}$ = 6.7 Hz, H$_\alpha$-PyRe), 8.52 (d, 4 H, $^3J_{H-H}$ = 6.1 Hz, H$_\alpha$-Py), 7.42 (d, 4 H, $^3J_{H-H}$ = 6.3 Hz, H$_\beta$-PyRe), 7.13−7.08 (m, 6 H, H$_\beta$-Py, RePyC*H*=CHPy), 6.89 (d, 2 H, $^3J_{H-H}$ = 12.2 Hz, RePyCH=C*H*Py).

General Procedure for the Synthesis of the Square Complexes. To a 100 mL flask containing 0.1 mmol of [M(dppf)$(H_2O)_2$](OTf)$_2$ (M = Pd or Pt) and 0.1 mmol of *fac*-BrRe(CO)$_3$(L)$_2$ (L = AZP or BPE) was added 30 mL of dried CH_2Cl_2, and the resulting mixture was stirred at room temperature in the dark under nitrogen for 24 h. The solution was added to 250 mL of cold ether, and the resulting precipitate was collected on a frit, washed with cold ether, and dried in vacuo.

Cyclobis{[*cis*-(dppf)Pd](*μ*-*trans*-AZP)$_2$(*fac*-Re(CO)$_3$Br)}(OTf)$_4$ (5). Yield: 88%. IR (ν_{CO}, cm^{-1}, CH_2Cl_2): 2029, 1933, 1898. ^{1}H NMR (acetone-d_6): 9.19 (br d, 8 H, H$_\alpha$-PyPd), 9.15 (d, 8 H, $^3J_{H-H}$ = 6.8 Hz, H$_\alpha$-PyRe), 8.03−7.97 (m, 16 H, H$_o$-PhP), 7.81 (d, 8 H, $^3J_{H-H}$ = 6.8 Hz, H$_\beta$-PyRe), 7.71−7.63 (m, 24 H, H$_{m,p}$-PhP), 7.45 (d, 8 H, $^3J_{H-H}$ = 5.9 Hz, H$_\beta$-PyPd), 4.92 (s, 8 H, H$_\alpha$-ferr), 4.81 (s, 8 H, H$_\beta$-ferr). ^{31}P NMR (acetone-d_6): 35.3 (s). ESI-MS: m/z = 1527.4 (calcd m/z = 1527.0 for [M − 2OTf$^-$]$^{2+}$). Anal. Calcd for $C_{118}H_{88}N_{16}Br_2O_{18}F_{12}P_4Fe_2S_4Pd_2Re_2$: C, 42.25; H, 2.64; N, 6.68. Found: C, 41.99; H, 2.54; N, 6.69.

Cyclo{[*cis*-(dppf)Pd](*μ*-cis-AZP)$_2$(*fac*-Re(CO)$_3$Br)}(OTf)$_2$ (6). Yield: 90%. IR (ν_{CO}, cm^{-1}, CH_2Cl_2): 2029, 1932, 1897. ^{1}H NMR (acetone-d_6): 9.13 (br d, 8 H, H$_\alpha$-PyPd), 9.09 (d, 8 H, $^3J_{H-H}$ = 6.8 Hz, H$_\alpha$-PyRe), 8.02−7.99 (m, 16 H, H$_o$-PhP), 7.73−7.61 (m, 32 H, H$_\beta$-PyRe, H$_{m,p}$-PhP), 7.04 (d, 8 H, $^3J_{H-H}$ = 5.8 Hz, H$_\beta$-PyPd), 4.91 (s, 8 H, H$_\alpha$-ferr), 4.79 (s, 8 H, H$_\beta$-ferr). ^{31}P NMR (acetone-d_6): 36.5 (s). ESI-MS: m/z = 1527.8 (calcd m/z = 1527.0 for [M − OTf$^-$]$^+$). Anal. Calcd for $C_{59}H_{44}N_8BrO_9F_6P_2FeS_2PdRe$: C, 42.25; H, 2.64; N, 6.68. Found: C, 41.77; H, 2.41; N, 6.93.

Cyclobis{[*cis*-(dppf)Pt](*μ*-trans-AZP)$_2$(*fac*-Re(CO)$_3$Br)}(OTf)$_4$ (7). Yield: 75%. IR (ν_{CO}, cm^{-1}, CH_2Cl_2): 2029, 1931, 1897. ^{1}H NMR (acetone-d_6): 9.24 (br d, 8 H, H$_\alpha$-PyPt), 9.16 (d, 8 H, $^3J_{H-H}$ = 6.8 Hz, H$_\alpha$-PyRe), 8.00 (m, 16 H, H$_o$-PhP), 7.82 (d, 8 H, $^3J_{H-H}$ = 6.8 Hz, H$_\beta$-PyRe), 7.68−7.61 (m, 24 H, H$_{m,p}$-PhP), 7.48 (d, 8 H, $^3J_{H-H}$ = 6.3 Hz, H$_\beta$-PyPt), 4.89 (s, 8 H, H$_\alpha$-ferr), 4.77 (s, 8 H, H$_\beta$-ferr). ^{31}P NMR (acetone-d_6): 5.36 (t, J_{Pt-P} = 3662 Hz). ESI-MS: m/z = 1028.1 (calcd m/z = 1027.7 for [M − 3OTf$^-$]$^{3+}$). Anal. Calcd for $C_{118}H_{88}N_{16}Br_2O_{18}F_{12}P_4Fe_2S_4Pt_2Re_2$: C, 40.12; H, 2.51; N, 6.34. Found: C, 39.74; H, 2.76; N, 6.69.

Cyclobis{[*cis*-(dppf)Pd](*μ*-*trans*-BPE)$_2$(*fac*-Re(CO)$_3$Br)}(OTf)$_4$ (8). Yield: 85%. IR (ν_{CO}, cm^{-1}, acetone): 2024, 1922, 1892. ^{1}H NMR (CD_3NO_2): 8.81 (d, 8 H, $^3J_{H-H}$ = 6.5 Hz, H$_\alpha$-PyRe), 8.34 (br d, 8 H, H$_\alpha$-PyPd), 7.90 (m, 16 H, H$_o$-PhP), 7.73 (m, 8 H, H$_p$-PhP), 7.62 (m, 16 H, H$_m$-PhP), 7.47 (d, 8 H, $^3J_{H-H}$ = 6.5 Hz, H$_\beta$-PyRe), 7.31 (d, 4 H, $^3J_{H-H}$ = 16.4 Hz, C=C*H*Re), 7.24 (d, 8 H, $^3J_{H-H}$ = 5.7 Hz, H$_\beta$-PyPd), 7.20 (d, 4 H, $^3J_{H-H}$ = 16.3 Hz, C=C*H*Pd), 4.78 (s, 8 H, H$_\alpha$-ferr), 4.72 (s, 8 H, H$_\beta$-ferr). ^{31}P NMR (CD_3NO_2): 36.8 (s). ESI-MS: m/z = 3196.0 (calcd m/z = 3194.9 for [M − OTf$^-$]$^+$). Anal. Calcd for $C_{126}H_{96}N_8Br_2O_{18}F_{12}P_4Fe_2S_4Pd_2Re_2$: C, 45.22; H, 2.89; N, 3.35. Found: C, 45.16; H, 2.72; N, 3.07.

Cyclo{[*cis*-(dppf)Pd](*μ*-*cis*-BPE)$_2$(*fac*-Re(CO)$_3$Br)}(OTf)$_2$ (9). Complex **4** was irradiated at 366 nm in CH_2Cl_2 for 1 h before an equimolar amount of *cis*-(dppf)Pd$(H_2O)_2$(OTf) was added to the solution. The workup procedures are essentially the same as those of square **8**. Yield: 83%. IR (ν_{CO}, cm^{-1}, acetone): 2022, 1921, 1892. ^{1}H NMR (CD_3NO_2): 8.65 (br d, 4 H, H$_\alpha$-PyPd), 8.60 (d, 4 H, $^3J_{H-H}$ = 6.6 Hz, H$_\alpha$-PyRe), 7.94−7.56 (m, 20 H, H$_{o,m,p}$-PhP), 7.44 (d, 4 H, $^3J_{H-H}$ = 6.6 Hz, H$_\beta$-PyRe), 7.22 (d, 4 H, $^3J_{H-H}$ = 5.7 Hz, H$_\beta$-PyPd), 7.10 (d, 2 H, $^3J_{H-H}$ = 12.1 Hz, C=C*H*Re), 6.92 (d,

(7) (a) Schanze, K. S.; Lucia, L. A.; Cooper, M.; Walters, K. A.; Ji, H.-F.; Sabina, O. *J. Phys. Chem. A* **1998**, *102*, 5577. (b) Sun, S.-S.; Robson, E.; Dunwoody, N.; Silva, A. S.; Brinn, I. M.; Lees, A. J. *Chem. Commun*. **2000**, 201. (c) Lewis, J. D.; Perutz, R. N.; Moore, J. N. *Chem. Commun*. **2000**, 1865. (d) Fernandez-Acebes, A.; Lehn, J.-M. *Chem. Eur. J*. **1999**, *5*, 3285. (e) Wrighton, M. S.; Morse, D. L.; Pdungsap, L. *J. Am. Chem. Soc*. **1975**, *97*, 2073. (f) Zarnegar, P. P.; Bock, C. R.; Whitten, D. G. *J. Am. Chem. Soc*. **1973**, *95*, 4367. (g) Itokazu, M. K.; Polo, A. S.; de Faria, D. L. A.; Bignozzi, C. A.; Iha, N. Y. M. *Inorg. Chim. Acta* **2001**, *313*, 149. (h) Pdungsap, L.; Wrighton, M. S. *J. Organomet. Chem.* **1977**, *127*, 337. (i) Sun, S.-S.; Lees, A. J. *Organometallics* **2002**, *21*, 39.

(8) Stang, P. J.; Olenyuk, B.; Fan, J.; Arif, A. M. *Organometallics* **1996**, *15*, 904.

(9) (a) Slone, R. V.; Benkstein, K. D.; Bélanger, S.; Hupp, J. T.; Guzei, I. A.; Rheingold, A. L. *Coord. Chem. Rev*. **1998**, *171*, 121. (b) Slone, R. V.; Yoon, D. I.; Calhoun, R. M.; Hupp, J. T. *J. Am. Chem. Soc*. **1995**, *117*, 11813.

(10) Brown, E. V.; Granneman, G. R. *J. Am. Chem. Soc*. **1975**, *97*, 621.

(11) (a) Whitten, D. G.; McCall, M. T. *Tetrahedron Lett*. **1968**, 2759. (b) Ebbesen, T. W.; Previtali, C. M.; Karatsu, T.; Arai, T.; Tokumaru, K. *Chem. Phys. Lett*. **1985**, *119*, 489.

(12) Vitali, D.; Calderazzo, F. *Gazz. Chim. Ital*. **1972**, *102*, 587.

Scheme 1

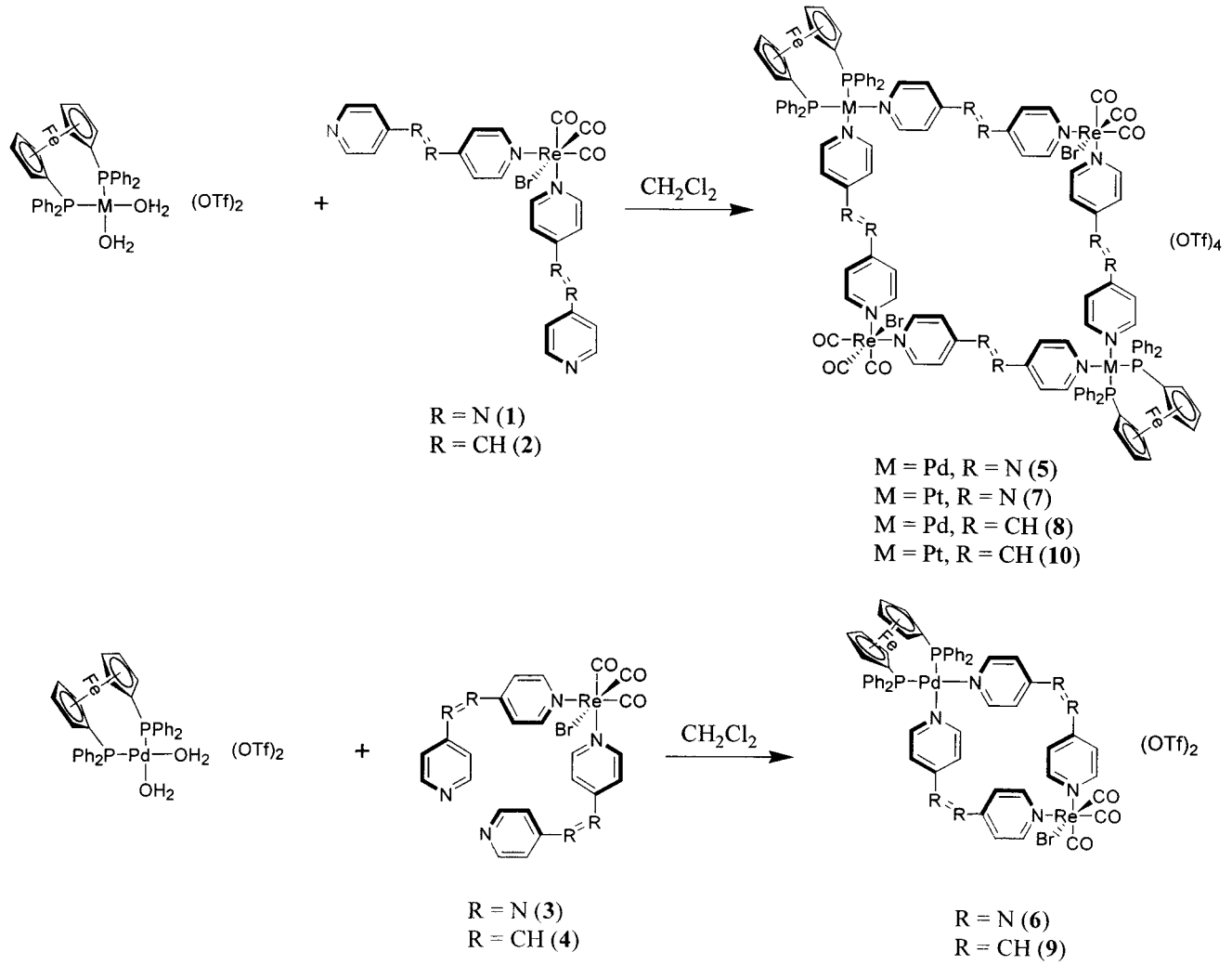

2 H, $^3J_{H-H}$ = 12.3 Hz, C=C*H*Pd), 4.78 (s, 4 H, H_α-ferr), 4.70 (s, 4 H, H_β-ferr). ^{31}P NMR (CD_3NO_2): 36.8 (s). ESI-MS: *m*/*z* = 1522.0 (calcd *m*/*z* = 1523.0 for [M − OTf^-]$^+$). Anal. Calcd for $C_{63}H_{48}N_4BrO_9F_6P_2FeS_2PdRe$: C, 45.22; H, 2.89; N, 3.35. Found: C, 45.01; H, 2.99; N, 3.47.

Cyclobis{[*cis*-(dppf)Pt](*μ*-*trans*-BPE)$_2$(fac-Re(CO)$_3$Br)}-(OTf)$_4$ (10). Yield: 83%. IR (ν_{CO}, cm^{-1}, acetone): 2024, 1923, 1893. ^{1}H NMR (acetone-d_6): 8.90 (d, 8 H, $^3J_{H-H}$ = 6.6 Hz, H_α-PyRe), 8.80 (br d, 8 H, H_α-PyPd), 7.93 (m, 16 H, H_o-PhP), 7.67−7.55 (m, 36 H, $H_{m,p}$-PhP, C=C*H*Re, H_β-PyRe), 7.40 (d, 4 H, $^3J_{H-H}$ = 16.5 Hz, C=C*H*Pd), 7.32 (d, 8 H, $^3J_{H-H}$ = 6.7 Hz, H_β-PyPd), 4.83 (s, 8 H, H_α-ferr), 4.73 (s, 8 H, H_β-ferr). ^{31}P NMR (acetone-d_6): 5.20 (t, J_{Pt-P} = 3524 Hz). ESI-MS: *m*/*z* = 3374.1 (calcd *m*/*z* = 3373.0 for [M − OTf^-]$^+$). Anal. Calcd for $C_{126}H_{96}N_8Br_2O_{18}F_{12}P_4Fe_2S_4Pt_2Re_2$: C, 42.94; H, 2.75; N, 3.18. Found: C, 43.84; H, 2.16; N, 2.97.

[*cis*-(dppf)Pd(*μ*-*trans*-AZP)]$_4$(OTf)$_8$ (11). To a 25 mL flask were added (dppf)Pd(H_2O)$_2$(OTf)$_2$ (99.5 mg, 0.1 mmol), *trans*-AZP (18.4 mg, 0.1 mmol), and 10 mL of N_2-degassed CH_2Cl_2. The resulting mixture was stirred at room temperature in the dark for 20 h. The purple precipitate was collected on a frit, washed with ether, and dried in vacuo. Yield: 73%. ^{1}H NMR (DMSO-d_6): 8.99 (br d, 16 H, H_α-Py), 7.79−7.53 (m, 96 H, $H_{o,m,p}$-PhP, H_β-Py), 4.81 (s, 16 H, H_α-ferr), 4.72 (s, 16 H, H_β-ferr). ^{31}P NMR (DMSO-d_6): 36.9 (s). ESI-MS: *m*/*z* = 2135.8 (calcd *m*/*z* = 2134.9 for [M − $2OTf^-$]$^{2+}$). Anal. Calcd for $C_{184}H_{144}N_{16}O_{24}F_{24}P_8Fe_4S_8Pd_4$: C, 48.33; H, 3.17; N, 4.90. Found: C, 48.55; H, 3.05; N, 4.99.

[*cis*-(dppf)Pd(*μ*-*cis*-AZP)]$_2$(OTf)$_4$ (12). The preparation of square **12** is essentially the same as that of square **11**. Yield: 82%. ^{1}H NMR (DMSO-d_6): 8.83 (br d, 8 H, H_α-Py), 7.75−7.56 (m, 40 H, $H_{o,m,p}$-PhP), 7.12 (d, 8 H, $^3J_{H-H}$ = 5.9 Hz, H_β-Py), 4.80 (s, 8 H, H_α-ferr), 4.70 (s, 8 H, H_β-ferr). ^{31}P NMR (DMSO-d_6): 36.5 (s). ESI-MS: *m*/*z* = 2133.8 (calcd *m*/*z* = 2135.0 for [M − OTf^-]$^+$). Anal. Calcd for $C_{92}H_{72}N_8O_{12}F_{12}P_4Fe_2S_4Pd_2$: C, 48.33; H, 3.17; N, 4.90. Found: C, 48.76; H, 3.39; N, 5.08.

Equipment and Procedures. ^{1}H NMR spectra were obtained using a Brücker AC 300 spectrometer or a Brücker AM 360 spectrometer. ^{13}C and ^{31}P NMR spectra were obtained using a Brücker AM 360 spectrometer. ESI-MS experiments were performed on a Finnigan MAT TSQ700 triple quadrupole mass spectrometer equipped with a Finnigan electrospray interface. Infrared spectra were measured on a Nicolet 20SXC Fourier transform infrared spectrophotometer. UV−vis spectra were obtained using an HP 8450A diode array spectrophotometer interfaced to an IBM computer. Emission spectra were recorded in deoxygenated solvent solution at 293 K with an SLM 48000S lifetime fluorescence spectrophotometer equipped with a red-sensitive Hamamatsu R928 photomultiplier tube. Irradiations at 313 and 366 nm were carried out with light from an Oriel Instruments 450 W mercury arc lamp using interference filters (Ealing Corp., 10 nm

Scheme 2

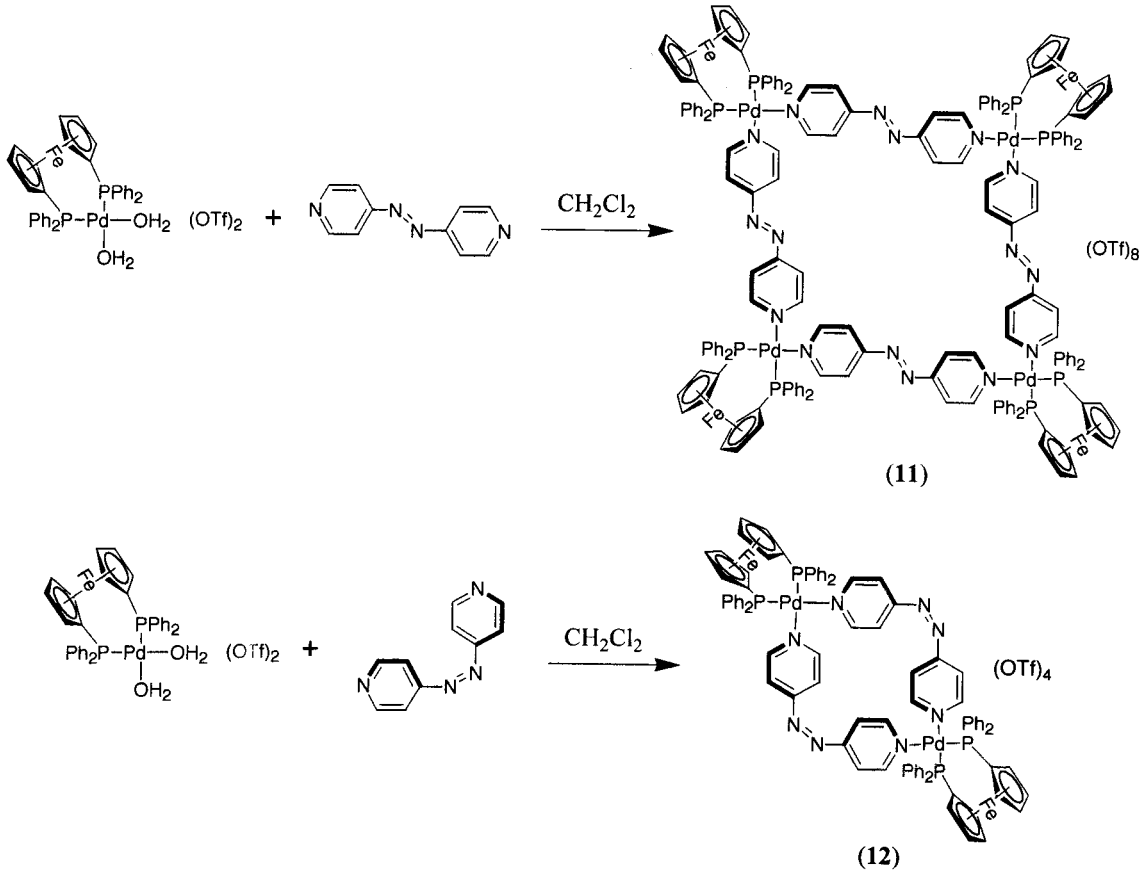

band-pass) to isolate the excitation wavelength. Incident light intensities were determined by Aberchrome 540 and ferrioxalate actinometry. The typical light intensity was 5×10^{-8} to 1×10^{-7} einstein/min. The resultant quantum efficiency values were determined for at least three readings on the basis of the first 10% conversion of the reaction and were found to be reproducible to within ±10% in all cases. Photostationary composition and conversion percentages for each compound were determined by integration of the peak areas in the ^{31}P NMP or ^{1}H NMR spectra recorded before and after irradiation in CD_2Cl_2 or CD_3CN.[13] Detailed procedures for the photophysical and photochemical measurements have been reported in previous papers.[6a,14]

Results and Discussion

Synthesis and Characterization. Schemes 1 and 2 illustrate the procedures used for preparation of the macrocyclic squares **5**−**12**. Tetranuclear squares **5**, **7**, **8**, and **10** were prepared from self-assembly of *trans* corner components *fac*-BrRe(CO)$_3$(*trans*-AZP)$_2$ or *fac*-BrRe(CO)$_3$(*trans*-BPE)$_2$ and (dppf)M(O$_2$H)$_2$(OTf)$_2$ (M = Pd or Pt) in CH_2Cl_2.[9] Dinuclear squares **6** and **9** were prepared by self-assembly of the *cis* corner components *fac*-BrRe(CO)$_3$(*cis*-AZP)$_2$ or *fac*-BrRe(CO)$_3$(*cis*-BPE)$_2$ and (dppf)Pd(O$_2$H)$_2$(OTf)$_2$ in CH_2Cl_2.[9] Squares **11** and **12** were prepared by self-assembly of (dppf)Pd(O$_2$H)$_2$(OTf)$_2$ and *trans*-AZP or *cis*-AZP in CH_2Cl_2, respectively.[8,15] Typical yields for the synthesis of these square complexes are greater than 70%, which are characteristic of thermodynamically driven self-assembly processes.[1] All of these compounds have been characterized by IR, ^{1}H NMR, ^{31}P NMR, electrospray ionization mass spectrometry (ESI-MS), and satisfactory elemental analyses, and these data all support the formation of tetranuclear or dinuclear square complexes. Attempts to synthesize the dinuclear squares containing the *cis*-(dppf)Pt moiety were unsuccessful. These squares do not form under the same experimental conditions as the dinuclear squares containing the *cis*-(dppf)Pd moiety. In these cases, prolonging the reaction time or heating the solution resulted in the formation of either a mixture of unidentified products or only the tetranuclear squares.

Electronic Absorption Spectra. The absorption spectral data obtained from all the squares, corner complexes, and free ligands are summarized in Table 1. Figure 1 compares the absorption spectra of the *trans*-AZP-linked square **5** and corner **1** as well as the *cis*-AZP-linked square **6** and corner **3** in CH_2Cl_2. The absorption spectra of *trans*-AZP and *cis*-AZP are also included for comparison. In general, the absorption spectra of AZP-containing squares and corner complexes feature intense bands in the UV region lower than 300 nm, and these are assigned to the AZP-localized $\pi-\pi^*$ transitions. A broad shoulder with a maximum around 380

(13) Bencini, A.; Bernardo, M. A.; Bianchi, A.; Ciampolini, M.; Fusi, V.; Nardi, N.; Parola, A.-J.; Pina, F.; Valtancoli, B. *J. Chem. Soc., Perkin Trans. 2* **1998**, 413.

(14) Dunwoody, N.; Sun, S.-S.; Lees, A. J. *Inorg. Chem*. **2000**, *39*, 4442.

(15) Stang, P. J.; Cao, D. H.; Saito, S.; Arif, A. M. *J. Am. Chem. Soc*. **1995**, *117*, 6273.

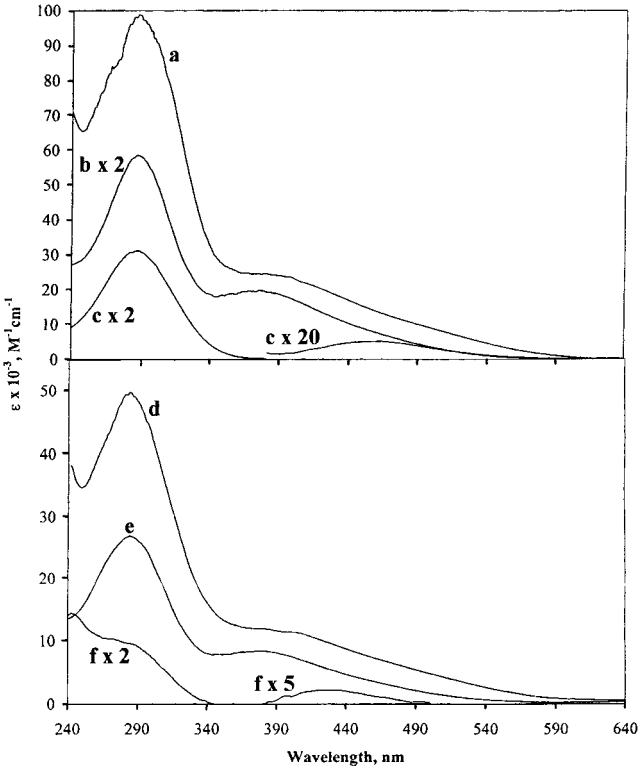

Figure 1. UV−vis absorption spectra of square **5** (curve a), corner **1** (curve b), *trans*-AZP (curve c), square **6** (curve d), corner **3** (curve e), and *cis*-AZP (curve f) in CH_2Cl_2 at 293 K.

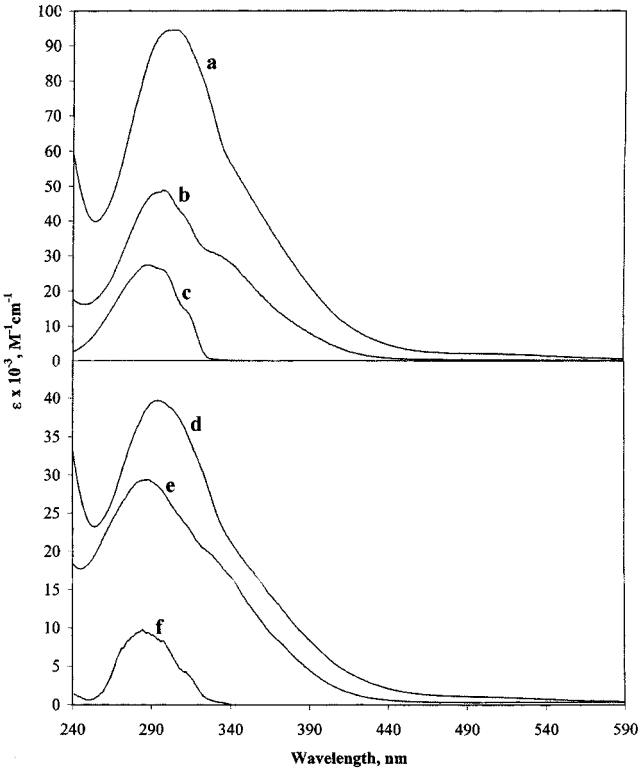

Figure 2. UV−vis absorption spectra of square **8** (curve a), corner **2** (curve b), *trans*-BPE (curve c), square **9** (curve d), corner **4** (curve e), and *cis*-BPE (curve f) in CH_2Cl_2 at 293 K.

Table 1. Absorption Spectral Data in CH_2Cl_2 at 293 K

compd	λ_{max}, nm ($10^{-3}\epsilon$, M^{-1} cm^{-1})
trans-AZP	288 (15.5), 462 (0.258)
cis-AZP	248 (6.89), 285 (sh, 4.81), 436 (0.433)
trans-BPE	287 (27.4), 299 (sh, 25.3), 311 (sh, 14.8)
cis-BPE	284 (11.6)
1	285 (29.3), 376 (10.0)
2	297 (48.8), 340 (sh, 27.8)
3	284 (26.9), 378 (8.42)
4	287 (29.4), 330 (sh, 19.0)
5	288 (98.7), 380 (24.5)
6	284 (49.7), 414 (10.7)
7	275 (115), 396 (28.5)
8	304 (94.5), 360 (sh, 33.4), 498 (2.14)
9	294 (39.7), 504 (1.04)
10	306 (87.4), 360 (sh, 26.1)
11	282 (106), 370 (12.4), 552 (3.77)
12	277 (51), 351 (sh, 14.1), 514 (2.00)

nm for each of the AZP-bridged squares and corner complexes is assigned to Re(dπ) → AZP (π*) metal-to-ligand charge transfer (MLCT).[6a] The very weak absorption band that tails into the visible region comprises AZP-localized n−π*,[6h,10] Pd-centered ligand-field (LF),[16] and Fe-centered LF[17] absorptions. The absorption spectra of **11** and **12** comprise a series of ligand-localized $\pi-\pi$*, Pd(dπ) → AZP (π*) MLCT, Pd-centered ligand-field, AZP-localized n−π*, and Fe-centered ligand-field absorptions. No luminescence was observed from any AZP-bridged squares or corner complexes in room temperature CH_2Cl_2 or CH_3CN solution. The proximity of close-lying Pd- and Fe-localized ligand-field bands to the lowest excited state(s) is understood to contribute to the lack of emission observed from the photoproduct and provide an efficient pathway where the excited state is rapidly converted by nonradiative decay to the ground state.[9b,16,18]

Figure 2 shows the absorption spectra of the *trans*-BPE-linked square **8** and corner **2** as well as *cis*-BPE-linked square **9** and corner **4** in CH_2Cl_2 solution. The absorption spectra of *trans*-BPE and *cis*-BPE ligands are also included for comparison. The absorption spectra of *trans*-BPE-containing squares and corner complexes feature an intense band around 300 nm that extends into the visible region. The band maximum slightly shifts to around 290 nm in *cis*-BPE-bridged squares and corner complexes. This band is tentatively assigned to overlapping BPE-localized $\pi-\pi$*, Re(dπ) → BPE (π*), and Pd(dπ) (or Pt) → BPE (π*) MLCT transitions. Square **8** also features a weak absorption at 524 nm that is assigned to overlapping Pd-centered and Fe-centered LF transitions. Again, no luminescence was observed from any of the BPE-bridged squares or corner complexes in room temperature CH_2Cl_2 solution.

Photoisomerization of *trans*-AZP-Containing Squares and Corner Complexes. Upon irradiation of **5** at 313 nm in 293 K CH_2Cl_2 solution, the bands at 288 and 380 nm gradually decrease and the band at 504 nm slowly increases (see Figure 3A). Due to the significant band overlap between the $\pi-\pi$* transitions localized on AZP and dppf, the spectral changes are not as prominent as in the case of free AZP or

(16) Lai, S.-W.; Cheung, T.-C.; Chan, M. C. W.; Cheung, K.-K.; Peng, S.-M.; Che, C.-M. *Inorg. Chem.* **2000**, *39*, 255.
(17) Sohn, Y. S.; Hendrickson, D. N.; Gray, H. B. *J. Am. Chem. Soc.* **1971**, *28*, 3603.
(18) Yam, V. W.-W.; Lee, V. W.-M.; Cheung, K.-K. *Organometallics* **1997**, *16*, 2833.

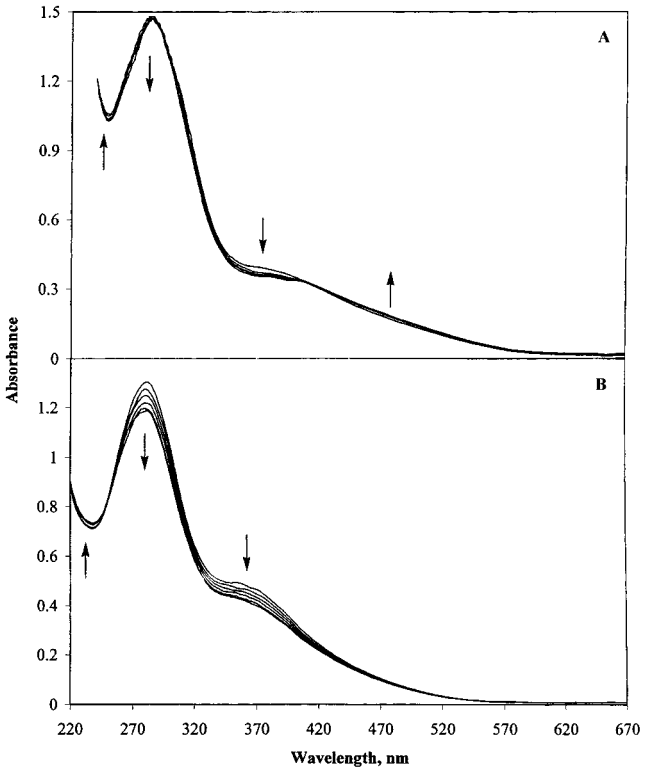

Figure 3. UV−vis absorption spectral changes observed from square **5** (A) and corner **1** (B) upon photolysis at 313 nm in CH_2Cl_2 at 293 K.

corner **1** (see Figure 3B). Nevertheless, the spectral changes apparently indicate a *trans*−*cis* isomerization of the AZP ligand, as evidenced by the small growth of the visible band, which is characteristic of *cis*-azo compounds,[19] as well as by the appearance of the peak belonging to the dinuclear square **6** in the ^{31}P NMR spectrum. After 24 h of irradiation, a photostationary state was reached where the **5**:**6** ratio was 3:2 on the basis of the ^{31}P NMR data. The mixture of tetramers and dimers can be fully converted back to pure tetramers by heating the solution at 323 K in the dark for 3 h. All this evidence supports the isomerization behavior between the tetranuclear species and the dinuclear species (see Scheme 3). Although we do not have exact formation constants between the Pd(II) (or Pt(II)) and pyridine, the thermodynamic stability of all the squares suggests that these should be extremely large. However, the labile nature of the Pd(II) center also tells us that the equilibrium between the coordination and uncoordination of Pd(II)−py processes should be very fast and that isomerization would be more favorable through the uncoordinated site due to the lack of strain arising from a twisting of the Pd(II)−N bond, i.e., dissociation of Pd(II)−py first and then isomerization. It should be noted that the tetramer−dimer interconversions were entirely reproducible; the same spectral results were obtained even when they were repeated several times for an individual solution.

In contrast, square **7** exhibits only a slow disassembly of the square structure and the formation of (dppf)Pt$(OTf)_2$ and *fac*-BrRe$(CO)_3$(*cis*-AZP)$_2$ in solution upon irradiation at either 366 or 313 nm. The lack of tetramer−dimer transformation is associated with the less labile nature of the Pt−N bond compared to the Pd−N bond in room temperature solution.[20] The large strain imposed on the square structure results in disassembly when the *trans*-AZP complex converts to its *cis*-isomer. A similar photoinduced disassembly of an AZP-bridged square complex, [*fac*-Cl$(CO)_3$Re(μ-AZP]$_4$, has been previously observed.[6a] However, the molecular components *fac*-BrRe$(CO)_3$(*cis*-AZP)$_2$ and (dppf)Pt$(OTf)_2$ do not completely self-assemble into the dinuclear square even after the solution is stirred at room temperature for 3 days. The obtained ^{1}H NMR spectrum shows structurally unidentified peaks, and there are at least three different species existing in solution on the basis of the ^{31}P NMR spectrum. Nevertheless, square **7** was still fully recovered by heating the solution at 323 K for 48 h.

Table 2. Quantum Efficiencies (Φ) of Photoinduced Isomerization of Squares and Their Re(I) Corner Complexes at 293 K[a]

	366 nm		313 nm	
compd	Θ	% *cis*[b]	Θ	% *cis*[b]
1	0.092	78	0.088	78
3	0.32	95	0.30	90
5	0.036	50	0.0097	40
7[c]	0.048		0.017	
8	0.044	83	0.035	80
10[c]	0.11		0.094	
11	0.040	67	0.023	60

[a] The photolysis experiments were conducted in deoxygenated CH_2Cl_2 solution except for those of square **11**, which were performed in deoxygenated CH_3CN solution. [b] At the photostationary state. [c] Quantum efficiency of the disassembly of the square structure.

A photoinduced isomerization similar to that described above was observed when **11** was photolyzed at 313 nm in 293 K CH_3CN solution. In the absorption spectrum, the band at 282 nm slowly decreases and blue-shifts to 270 nm on irradiation, while the band at 370 nm slowly increases and reaches a photostationary state after 20 h of photolysis. In this case a tetramer:dimer ratio of 2:3 was observed, as evidenced by ^{31}P NMR data. The same rationalization described above for **5** is also applicable here to **11**. Similarly, the mixture of tetranuclear **11** and dinuclear **12** fully converted back to the tetranuclear species following heating at 323 K for 1 h.

Table 2 summarizes the quantum efficiencies at excitation wavelengths 366 and 313 nm of the bridging ligand *trans*−*cis* isomerization or disassembly of the square structure as well as the compositions at the photostationary state. In general, the quantum efficiencies at 366 nm are higher than the ones at 313 nm, and the quantum efficiencies of the corner **1** are higher than the quantum efficiencies of squares **5**, **7**, and **11**. These observations are ascribed to the presence of the $\pi-\pi^*$ transition localized on dppf and the LF bands localized on ferrocene, which act as an energy sink to dissipate the excited-state energy at the higher excitation wavelength.

(19) Kumar, G. S.; Neckers, D. C. *Chem. Rev.* **1989**, *89*, 1915.

(20) (a) Fujita, M.; Yazaki, J.; Ogura, K. *Chem. Lett*. **1991**, 1031. (b) Fujita, M.; Ibukuro, F.; Yamaguchi, K.; Ogura, K. *J. Am. Chem. Soc*. **1995**, *117*, 4175. (c) Ibukuro, F.; Kusukawa, T.; Fujita, M. *J. Am. Chem. Soc*. **1998**, *120*, 8561.

Scheme 3

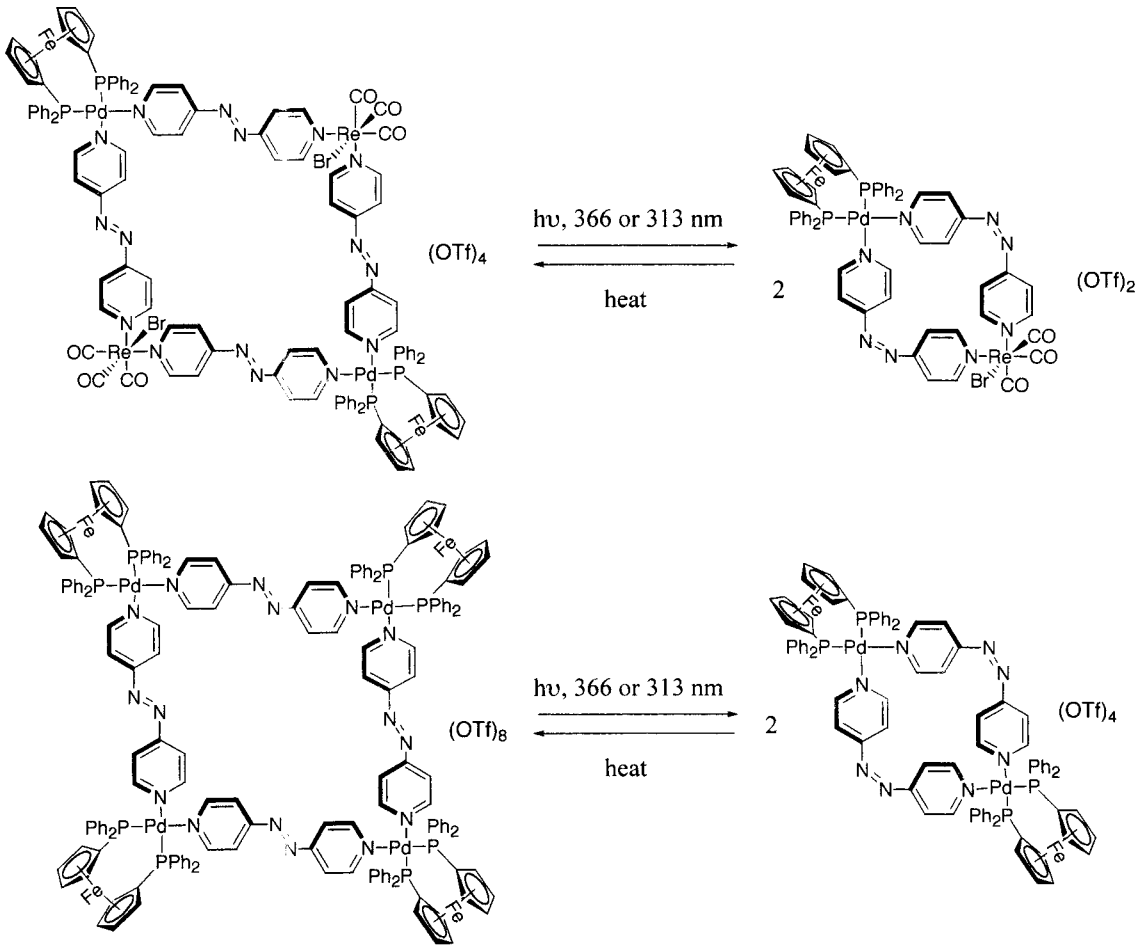

Photoisomerization of *trans*-BPE-Containing Squares and Corner Complexes. The *trans*-BPE free ligand has been shown to have a very low quantum efficiency ($\Phi = 0.003$ in benzene, 313 nm) for *trans*−*cis* isomerization upon direct irradiation in the absence of triplet sensitizers,[11a] which is in contrast to the efficient *trans*−*cis* photoisomerization of *trans*-stilbene ($\Phi = 0.52$ in pentane, 313 nm)[21] and *trans*-4-styrylpyridine ($\Phi = 0.38$ in CH_2Cl_2, 313 nm).[7e] The lack of direct irradiation *trans*−*cis* isomerization of BPE in the absence of a triplet sensitizer suggests that the isomerization of BPE occurs primarily through the triplet excited state.[22] Irradiation of square **8** or its corresponding corner **2** in CH_2Cl_2 solution at 366 or 313 nm resulted in a slow decrease of the lowest energy bands and an increase of the high-energy bands with clear isosbestic points at 277 and 269 nm for **8** and **2**, respectively.

Figure 4 compares the photolysis sequences of square **8** and corner **2** in CH_2Cl_2 at 313 nm. The spectral changes upon irradiation reflect the *trans*−*cis* isomerization of the bridging ligand. ^{1}H and ^{31}P NMR analyses indicate that the resulting photoproducts from **8** and **2** are cyclo[(dppf)Pd(μ-*cis*-BPE)$_2$Re(CO)$_3$Br](OTf)$_2$ (**9**) and *fac*-BrRe(CO)$_3$(*cis*-BPE)$_2$ (**4**), respectively, and the conversions are higher than 80% for both compounds at their photostationary states (see Scheme 4). The quantum yields at 366 and 313 nm for **8** or **2** are found to be wavelength independent, within experimental error; this implies that the photoisomerization occurs through the lowest $^3\pi\pi^*$ excited state localized at the olefinic double bond. In addition, the quantum yields of the corner **2** complex are higher than those of the square **8** at both wavelengths. These results are not totally unexpected given the fact that the low-lying LF states localized in the ferrocenyl moieties and Pd also function as energy sinks in square **8**. It is also noted that both isomerization processes for square **8** and corner **2** are fully reversible and that the *trans*-isomers can be recovered after the solution is stirred at 323 K for 24 h.

Irradiation of square **10** in CH_2Cl_2 solution at either 366 or 313 nm resulted in disassembly of the square structure into its Re(I) and Pt(II) corners, as evidenced by the changes observed in the ^{31}P NMR spectra and the absorption spectrum. The quantum efficiencies for the photoinduced disassembly process are 0.11 at 366 nm and 0.094 at 313 nm (Table 2). Again, there is no clear excitation wavelength dependence in the photoprocess. Similar to the case of square **7**, the molecular components BrRe(CO)$_3$(*cis*-BPE)$_2$ and (dppf)Pt(OTf)$_2$ do not completely self-assemble into the dinuclear square, even if the solution is allowed to stir at room temperature for 3 days, but the square **10** can be fully

(21) Saltiel, J.; Chang, D. W.-L.; Megarity, E. D. *J. Am. Chem. Soc*. **1974**, *96*, 6521.
(22) Gutiérrez, A. R.; Whitten, D. G. *J. Am. Chem. Soc*. **1974**, *96*, 7128.

Scheme 4

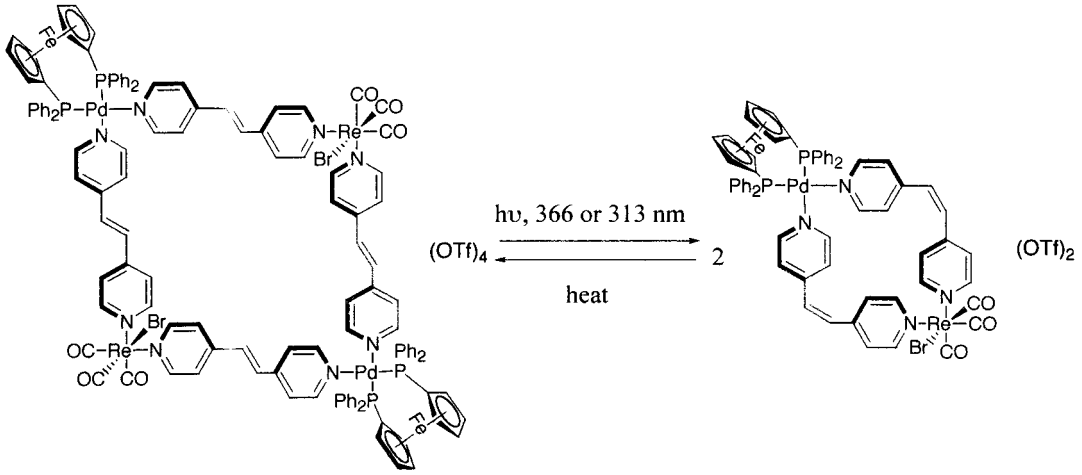

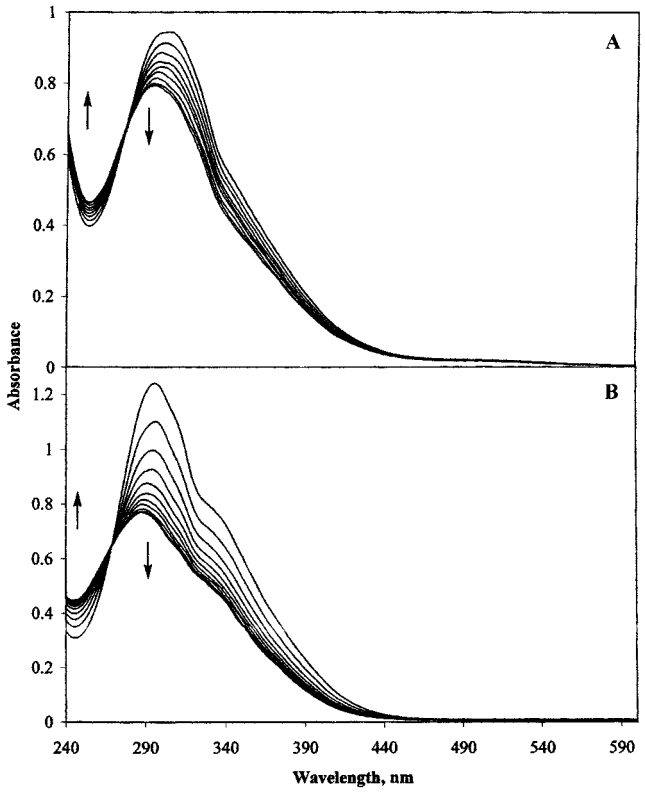

Figure 4. UV−vis absorption spectral changes observed from square **8** (A) and corner **2** (B) upon photolysis at 313 nm in CH_2Cl_2 at 293 K.

recovered by heating the solution at 323 K for 24 h. The different behavior between square **10** and its Pd(II) counterpart, square **8**, is again associated with the different lability toward the BPE ligand.[20] At room temperature, the less labile *cis*-(dppf)Pt requires a longer time to reach the most thermodynamic stable product (square) while the thermally driven isomerization of *fac*-$BrRe(CO)_3$(*cis*-BPE) takes place more readily. The result is the formation of a mixture comprising several different kinetic products. It is worth noting here that the kinetically stable square **10** can be forced to dissociate into its molecular components at room temperature by photoisomerization of the coordinating ligands.

Conclusion

We have successfully synthesized a series of self-assembly molecular squares bridged by a photoisomerizable ligand. The Pd−Re and Pd tetranuclear squares can be photochemically converted to their corresponding dinuclear squares and thermally returned back to the tetranuclear squares. The Pt−Re-based squares are not able to convert to their corresponding dinuclear squares. Instead, photoinduced disassembly of these squares was observed, although the disassembled components were able to self-assemble to their original square structures again upon heating.

Acknowledgment. We are grateful to the Division of Chemical Sciences, Office of Basic Energy Sciences, Office of Science, U.S. Department of Energy (Grant DE-FG02-89ER14039), for support of this research.

IC010998E